of ρ from the optimal value of 0.4563 is not expected to have unduly large adverse effect on stability: A decrease in ρ would actually improve TWF stability with a progressive destabilizing effect on the TSI, whereas the destabilization of TWF caused by an increase in ρ could be easily kept in check by increasing d slightly. To allow for possible inaccuracies in material properties, it is preferable to use the walls within a narrow velocity window just below the optimal conditions.

Materials suitable for the proposed walls are likely to be foam-based. These materials are lighter than water and possess a relatively high stiffness-to-weight ratio that renders them particularly effective against hydroelastic instabilities. The process of their manufacture influences their properties. They also offer the possibility of their properties being designed and manufactured to specification. Some variety may also offer very low damping because of their partially hollow nature (less material involved in straining). The bulk modulus of foam-based materials may theoretically be regulated by the pressure of the enclosed gas phase. With a view to the future development of materials technology, the construction of compliant coatings from foam-based polymeric materials cannot be ruled out. Navier's equations will be applicable to such materials if the cell size is much less than the wavelength of the perturbations.

The present study has focused on two-dimensional instability modes because these are known to be the most unstable for the TWF and SD. For the TSI, two-dimensional studies are still effective for comparing the relative stability performance of different isotropic compliant walls, although prediction on transition gain will be slightly reduced when three-dimensional modes are also considered.[11,12]

Conclusions

The present Note considers the optimization of single-layer viscoelastic compliant walls for delay of laminar-turbulent boundary-layer transition. The archetypal transition-delaying compliant layers should possess a nondimensional material density of 0.4563, elastic shear modulus of 0.5, and minimal material damping and should be sufficiently thick. The transition distances and transition delay factors obtained in the present study are comparable to the values reported by Dixon et al.[4] for their unit-density two-layer walls.

Acknowledgment

The results reported in this Note were obtained with the assistance of K. W. Lum.

References

[1]Carpenter, P. W., "Status of Transition Delay Using Compliant Walls," *Viscous Drag Reduction in Boundary Layers*, edited by D. M. Bushnell and J. N. Heffner, Vol. 123, Progress in Astronautics and Aeronautics, AIAA, Washington, DC, 1990, pp. 79–113.

[2]Riley, J. J., Gad-el-Hak, M., and Metcalfe, R. W., "Compliant Coatings," *Annual Review of Fluid Mechanics*, Vol. 20, 1988, pp. 393–420.

[3]Carpenter, P. W., Lucey, A. D., and Dixon, A. E., "The Optimization of Compliant Walls for Drag Reduction," *Recent Developments in Turbulence Management*, edited by K. S. Choi, Kluwer, Dordrecht, The Netherlands, 1991, pp. 195–221.

[4]Dixon, A. E., Lucey, A. D., and Carpenter, P. W., "Optimization of Viscoelastic Compliant Walls for Transition Delay," *AIAA Journal*, Vol. 32, No. 2, 1994, pp. 256–267.

[5]Yeo, K. S., "The Stability of Flow over Flexible Surfaces," Ph.D. Thesis, Dept. of Engineering, Univ. of Cambridge, Cambridge, England, UK, Nov. 1986.

[6]Yeo, K. S., "The Stability of Boundary-Layer Flow over Single- and Multi-Layer Viscoelastic Walls," *Journal of Fluid Mechanics*, Vol. 196, 1988, pp. 359–408.

[7]Yeo, K. S., and Dowling, A. P., "The Stability of Inviscid Flow over Passive Compliant Walls," *Journal of Fluid Mechanics*, Vol. 183, 1987, pp. 265–292.

[8]Yeo, K. S., Khoo, B. C., and Zhao, H. Z., "The Absolute Instability of Boundary-Layer Flow over Viscoelastic Walls," *Theoretical and Computational Fluid Dynamics*, Vol. 8, 1996, pp. 237–252.

[9]Smith, A. M. O., and Gamberoni, H., "Transition, Pressure Gradient and Stability Theory," Douglas Aircraft Co., Rept. ES26388, Long Beach, CA, 1956.

[10]Schubauer, G. B., and Skramstad, H. K., "Laminar Boundary-Layer Oscillations and Transition on a Flat Plate," NACA Rept. 909, 1948.

[11]Yeo, K. S., "The Three-Dimensional Stability of Boundary-Layer Flow over Compliant Walls," *Journal of Fluid Mechanics*, Vol. 238, 1992, pp. 537–577.

[12]Joslin, R. D., Morris, P. J., and Carpenter, P. W., "The Role of Three-Dimensional Instabilities in Compliant-Wall Boundary-Layer Transition," *AIAA Journal*, Vol. 29, No. 10, 1991, pp. 1603–1610.

J. Kallinderis
Associate Editor

Turbulence Structure in the Spiral Wake Shed by a Lifting Wing

Joseph A. Miranda* and William J. Devenport†
Virginia Polytechnic Institute and State University, Blacksburg, Virginia 24060

I. Introduction

THE wakes of large-aspect-ratio lifting wings are of great engineering and scientific interest. Much effort has been focused on understanding the tip vortices, but relatively little attention has been paid to the rest of the wake, specifically the axial wake of the wing boundary layers, and its development in the presence of the vortex. There have been several studies documenting the presence of this part of the wake and its evolving spiral form.[1–5] Of the most detail and of particular interest here is the work of Devenport et al.[1] Their measurements show the axial wake simultaneously decaying and rolling up around the vortex core, its turbulence structure evolving in the presence of lateral stretching, skewing, and lateral curvature. They show that, despite these complex and changing influences, the turbulence structure of this flow achieves an approximately self-similar state when normalized on the scale of the wake spiral and the axial velocity scale of the two-dimensional part of wake. This makes the flow of particular interest as an experimental and computational test case.

This Note summarizes a study[6] of a spiral wake similar to that of Devenport et al.[1] but in much greater detail. Our goal was to reveal precisely the effects of the different three-dimensional influences that act on the spiral wake and to compare its structure with the near-two-dimensional region found farther inboard. Both single- and two-point hot-wire measurements were made to this end. Single-point measurements are presented here; related two-point measurements and discussion relevant to aeroacoustic applications are dealt with in a companion paper.[7]

II. Apparatus and Instrumentation

The flow was generated in the $3 \times 2 \times 20$ ft test section of the Virginia Tech Subsonic Wind Tunnel using a rectangular planform, NACA 0012 half wing of 0.203-m chord c placed at 5-deg angle of attack. Flow in the empty test section is closely uniform, with a turbulence intensity of less than 0.3% (Ref. 8). A slight favorable streamwise pressure gradient $dC_p/dx = -0.96\%/\text{m}$ is present because of boundary-layer growth. The wing was mounted at the midheight of the test section and extended two thirds of the way across its 3-ft width. The wing boundary layers were tripped using 0.5-mm-diam glass beads glued in a random pattern between the

Presented as Paper 96-0804 at the AIAA 34th Aerospace Sciences Meeting, Reno, NV, Jan. 15–18, 1996; received June 5, 1997; revision received Nov. 25, 1997; accepted for publication Dec. 11, 1997.

*Graduate Research Assistant, Department of Aerospace and Ocean Engineering; currently Mechanical Engineer, U.S. Naval Undersea Warfare Center, Newport, RI 02847. Associate Member AIAA.

†Associate Professor, Department of Aerospace and Ocean Engineering, 215 Randolph Hall. Senior Member AIAA.

20 and 40% chord locations. Average density was 200 beads/cm^2. Velocity measurements were made using Auspex Corp. AVOP-4-100 four-sensor hot-wire probes. These probes, which consist of two orthogonal X-wire arrays with a total measurement volume of 0.5 mm^3, provide accurate and simultaneous measurements of all three velocity components with a frequency response in excess of 25 kHz (Ref. 9). They were operated using the instrumentation and procedures described by Devenport et al.[1] and Wittmer et al.[9] Helium bubble flow visualizations, described by Miranda and Devenport,[6] demonstrated that these probes could be used in and around the vortex core without significant interference effects.

III. Results and Discussion

Measurements were made 10 chord lengths downstream of the wing leading edge ($x/c = 10$) at a chord Reynolds number $U_\infty c/\nu$ of 3.2×10^5, corresponding to a freestream velocity U_∞ of some 26 m/s. Coordinates y (measured inboard from the center of the tip vortex) and z (measured from the vortex center in the direction of lift) are used to define positions relative to the vortex center in the crossflow plane y. Mean velocity components U, V, and W and fluctuations u, v, and w are defined in the directions of x, y, and z, respectively. Uncertainties in measured mean velocities are at worst 1.5% U_∞, e.g., at the vortex core edge, but typically much less. Uncertainties in turbulence stresses are typically $10^{-5}U_\infty^2$ near the centerline of the spiral wake and $2 \times 10^{-5}U_\infty^2$ in the vicinity of the vortex core.

Velocity measurements were made in a grid to provide a comprehensive cross-sectional view of the flowfield. Figure 1 shows contours of the turbulence kinetic energy k/U_∞^2 and mean streamwise vorticity $\omega_x c/U_\infty$ computed from these data. The structure of this lifting wake consists of a small concentrated vortex core surrounded by a circulating velocity field that winds the wing wake into an ever-increasing spiral. Detailed mean-velocity profiles through the core center showed it to have a radius of 3.9% c, a peak tangential velocity of 31% U_∞, and a centerline axial velocity deficit of 15% U_∞. Small-amplitude wandering of the vortex core was present of rms amplitude 0.35% c (~9% of the core radius) estimated using the method of Devenport et al.[1] Wandering of this amplitude would have had a negligible effect on mean velocity measurements[1] and would have contributed significantly only to turbulence stresses measured in the core region itself ($r < 0.06c$).

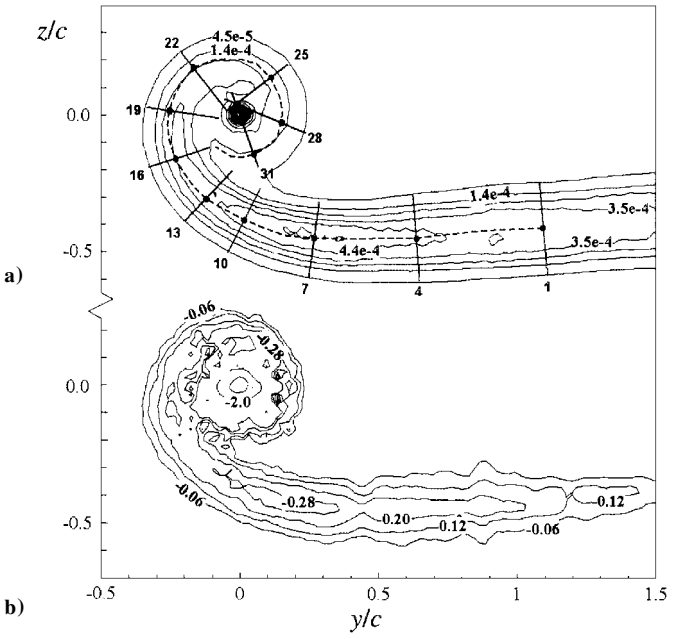

Fig. 1 Contours of a) turbulence kinetic energy with profile locations and numbers and wake centerline (– – –) and b) mean streamwise vorticity normalized on freestream velocity and chord length as appropriate.

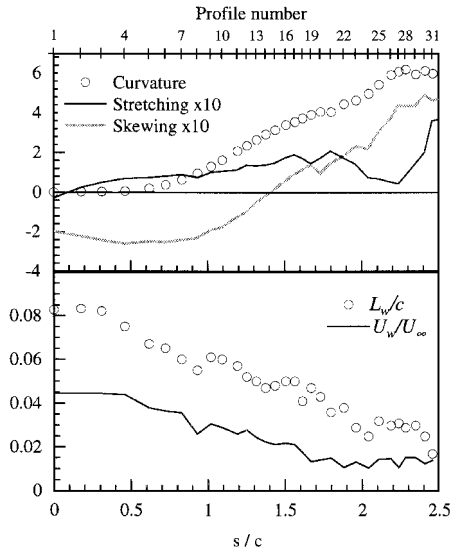

Fig. 2 Rates of lateral stretching $\partial V_s/\partial s$ and skewing $\partial V_s/\partial n$, lateral curvature of the wake centerline κ, mean axial velocity deficit at the wake centerline U_w, and half wake width L_w as functions of distance s along the centerline from profile 1. All results are normalized on U_∞ and c as appropriate.

Outside the core region, the turbulence structure is dominated by the axial wing wake. Far inboard, the wake is almost flat. Detailed measurements across the wake at $y/c = 1.1$ (Fig. 1a) show a Gaussian mean-velocity profile, an antisymmetric turbulence shear stress profile, and a double-peaked axial normal stress profile quantitatively similar to those of a two-dimensional plane wake.[10,11] Moving outboard toward the tip vortex, the wake first curves downward slightly and then upward as it wraps around the core. Turbulence levels in the wake rise as the wake begins to curve, reaching a maximum near $y/c = 0.2$, $z/c = -0.4$, but then fall as the core is approached. The variations in turbulence structure along the wake spiral can be attributed to a combination of its curvature and the additional strain rates it experiences in the velocity field generated by the vortex.

To accurately characterize these influences, a series of 31 velocity and turbulence stress profiles were measured across the spiral wake, as illustrated in Fig. 1a. The mean axial velocity profiles were used to determine the wake centerline (Fig. 1a), defined as the locus of minimum mean axial velocity. The lateral curvature of the centerline κ was computed by differentiation and is plotted in Fig. 2 in terms of distance along the centerline s and profile number. The rates of lateral stretching $\partial V_s/\partial s$ and skewing $\partial V_s/\partial n$ determined from the profile measurements also are plotted. Here, n and s are distances normal and parallel to the centerline, and V_n and V_s are the corresponding mean-velocity components. The curvature is essentially zero in the two-dimensional region (near profile 1) but increases rapidly as the wake winds around the core (profile locations 4 to 26). The curvature becomes approximately constant for the innermost part of the spiral (26 onward), indicating that the centerline is almost circular here. Near profile 1, the lateral stretching rate is also near zero but, as the spiral wake crosses the tangential velocity field of the vortex, it increases, reaching a maximum of about $0.2U_\infty/c$ around profile 22 and then falling away to reach a minimum around profile 27 in the circular part of the wake. The skewing rate is initially negative, increases through zero, and reaches its maximum positive values of about $0.47U_\infty/c$ closest to the core. The negative skewing far from the core is produced by the streamwise vorticity embedded in the wake here (Fig. 1b). The positive skewing is produced by the negative radial gradient of tangential velocity that surrounds the vortex.

Some of the effects of lateral curvature and secondary strain rates can be seen in Fig. 3, where velocity and turbulence stress profiles are plotted in terms of components resolved normal and parallel to the wake centerline. The mean profiles (Fig. 3a) clearly show the axial velocity deficit associated with the wake. Moving along the

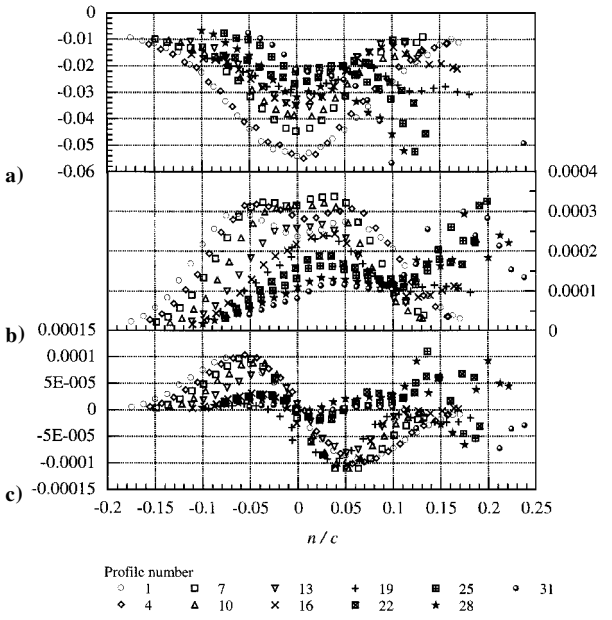

Fig. 3 Mean velocity and turbulence stress profiles through the wake resolved into components parallel and perpendicular to the wake centerline and normalized on U_∞ and c. Profile numbers are referenced to Fig. 1a: a) $(U - U_\infty)/U_\infty$, b) $\bar{u}^2/U_\infty^2$, and c) $\overline{uv_n}/U_\infty^2$.

spiral toward the vortex (from locations 1 to 31), both the width and the magnitude of the deficit decrease. Along the outer part of the spiral, the profiles remain fairly symmetric about the wake centerline (locations 1 to 16). Along the inner part, the profiles begin to overlap with the axial velocity deficit of the vortex core itself, which tends to drag down the positive n side of the profiles. Figure 2 summarizes these variations in terms of the centerline axial velocity deficit U_w and the half wake width L_w (determined from the negative n half of each profile). Ignoring the scatter, both fall monotonically and by a factor of about 3 as the wake wraps around the vortex.

This weakening of the wake clearly influences the turbulence stress profiles, all of which show much smaller stresses in the tightly wound part of the spiral wake than in the two-dimensional region (Figs. 3b and 3c). For the normal stress profiles, this fall is neither monotonic nor isotropic, however. As the vortex is approached, the normal stresses first rise to maxima near location 7 and then fall. The magnitude of the rise and subsequent fall is different depending on component, the variations tending to favor the axial and perpendicular-to-wake components $\bar{u}^2$ and $\bar{v}_n^2$ over the lateral component $\bar{v}_s^2$ ($\bar{v}_n^2$ and $\bar{v}_s^2$ are not shown). The consequent anisotropy is most pronounced around profile 22, where $\bar{v}_n^2$ is about three times $\bar{v}_s^2$, and $\bar{u}^2$ is about twice $\bar{v}_s^2$. Ultimately, at profile 31, the wake centerline values of $\bar{u}^2$, $\bar{v}_n^2$, and $\bar{v}_s^2$ have fallen to 0.3, 0.4, and 0.2 times their values in the two-dimensional part of the wake, respectively. The primary turbulence shear stress $\overline{uv_n}$ is at least 10 times smaller at profile 31 than at profile 1. All of the turbulence stress profiles measured in the inner part of the wake spiral (locations 19 onward) show some of the turbulence stress field associated with the vortex core and significant asymmetries apparently associated with the curvature of the wake. (Skewing and stretching should act symmetrically on both sides of the wake.) The crossflow shear stress $\overline{v_n v_s}$ profiles (not shown) show fairly large positive values in the region around profile 7, where the wake first becomes curved but becomes negative in the tightly wound region around the core. This variation appears to result from the rate of lateral skewing (Fig. 2), which also changes sign as the vortex is approached.

Despite the asymmetry produced by the wake curvature and the additional turbulence shear stresses generated by the skewing, the dramatic thinning and weakening of the wake as it is wound around the core suggest that lateral stretching has an important, if not dominant, effect on the turbulence structure of the spiral wake. Keffer[12] observed that lateral stretching of a two-dimensional wake caused the intensification of eddies aligned with the stretching direction, the attenuation of other large-scale motions, and an increase in the dissipation. These result in an increase in the intensity of velocity fluctuations perpendicular to the stretching direction compared to those parallel to the stretching, much as seen here.

IV. Conclusions

Velocity measurements have revealed in detail the structure of a spiral wake surrounding a wing-tip vortex. The tip vortex stretches, skews, and curves the wake. As the wake winds around the vortex, lateral stretching dramatically thins and weakens it, reducing the local wake half width L_w and peak axial velocity deficit U_w to about one third of their values in the two-dimensional region. The weakening of the wake influences turbulence stress profiles, all of which show much smaller stress levels in the tightly wound part of the spiral wake than in the two-dimensional region. The stretching also acts directly on the turbulence, producing significant anisotropy among the normal turbulence stresses. The damping effects of the stretching are to some small extent counteracted by skewing of the wake in the vortex tangential velocity field and under the action of its own embedded vorticity. The skewing gives rise to significant crossflow turbulence shear stress. Lateral curvature also plays a role, introducing asymmetry into the turbulence stress profile of the wake.

Acknowledgments

The authors would like to thank the Office of Naval Research (ONR), in particular L. Patrick Purtell, for their support under ONR Grant N00014-92-J4087 and Augmentation Awards for Science and Engineering Research Training Award N00014-94-1-0744. The full data set from this experiment is available from the authors.‡

References

[1]Devenport, W. J., Rife, M. C., Liapis, S. I., and Follin, G. J., "The Structure and Development of a Wing-Tip Vortex," *Journal of Fluid Mechanics*, Vol. 312, 1996, pp. 67–106.

[2]Mertaugh, L. J., Damania, R. B., and Paillet, F. L., "An Investigation of the Near-Field Wake Behind a Full-Scale Test Aircraft," *Journal of Aircraft*, Vol. 14, No. 9, 1977, pp. 894–902.

[3]Stinebring, D. R., Farrell, K. J., and Billet, M. L., "The Structure of a Three-Dimensional Tip Vortex at High Reynolds Numbers," *Journal of Fluids Engineering*, Vol. 113, Sept. 1991, pp. 496–503.

[4]Chow, J. S., Zilliac, G. G., and Bradshaw, P., "Turbulence Measurements in the Near Field of a Wing-Tip Vortex," American Society of Mechanical Engineers Forum on Complex Turbulent Flows, Chicago, IL, Nov. 1994.

[5]Zheng, Y., "An Experimental Study of Wing-Tip Vortex in the Near Wake of a Rectangular Wing," Ph.D. Thesis, School of Mechanical and Materials Engineering, Washington State Univ., Pullman, WA, 1992.

[6]Miranda, J. A., and Devenport, W. J., "The Structure of a Trailing Vortex Wake," Dept. of Aerospace and Ocean Engineering, Virginia Polytechnic Inst. and State Univ., Rept. VPI-AOE-233, Blacksburg, VA, May 1996.

[7]Devenport, W. J., Wenger, C. W., Glegg, S. A. L., and Miranda, J. A., "Wavenumber Frequency Spectra of Turbulence in a Lifting Wake for Broadband Noise Prediction," AIAA Paper 97-1699, May 1997.

[8]Engel, M. A., "A Wind-Tunnel Investigation of a Wing-Tip Trailing Vortex," M.S. Thesis, Dept. of Aerospace and Ocean Engineering, Virginia Polytechnic Inst. and State Univ., Blacksburg, VA, 1995.

[9]Wittmer, K. S., Devenport, W. J., and Zsoldos, J. S., "A Four Sensor Hot-Wire Probe System for Three-Component Velocity Measurement," *Experiments in Fluids* (to be published).

[10]Townsend, A. A., *The Structure of Turbulent Shear Flow*, Cambridge Univ. Press, Cambridge, England, UK, 1956, pp. 131–170.

[11]Wygnanski, I., Champagne, F., and Marasli, B., "On the Large Scale Structures in Two-Dimensional Small-Deficit Turbulent Wakes," *Journal of Fluid Mechanics*, Vol. 168, 1986, pp. 31–71.

[12]Keffer, J. F., "The Uniform Distortion of a Turbulent Wake," *Journal of Fluid Mechanics*, Vol. 22, 1965, pp. 135–159.

A. Plotkin
Associate Editor

‡Data may be accessed electronically at http://www.aoe.vt.edu/flowdata.